Bulletin of Earth Sciences of Thailand

The influence of pre-existing structures on fracture systems in the Jurassic Surat basin, Queensland, Australia

Sirirat Khamsaeng[1*], and Sukonmeth Jitmahantakul[2]

[1]Department of Geology, Faculty of Science,
Chulalongkorn University, Bangkok, 10330 Thailand
[2]M.Sc. Program in Energy Geoscience, Faculty of Science, Chulalongkorn University,
Bangkok, 10330, Thailand

* Corresponding author e-mail: khamsaeng.sirirat@gmail.com

Abstract

Pre-existing structures can influence the spatial distribution and geometry of subsequent fractures in sedimentary basins. In Queensland, Australia, contractional structures in the Permian-Triassic Bowen Basin control fracture development in the overlying Jurassic Surat Basin, where the Precipice sandstone is targeted for geological storage of carbon dioxide (CO_2). Understanding the influence of pre-existing structures in the Bowen Basin on fracture systems in the Surat Basin is vital for the site selection process of CO_2 geological storage projects in Queensland. This study focuses on the NW-SE trending Miles Thrust Fault (MTF) and its associated fault-propagation folds in the Bowen Basin, aiming to understand their influence on fracture systems in the overlying Jurassic succession of the Surat Basin. Results from 3D seismic interpretation and structural reconstruction reveal that the Surat Basin is characterized by localized extensional faults. These faults crest above the fault-propagation folds of the MTF and strike parallel to the NW-SE trending fold axis. An overlapping relay zone of the extensional faults occurs above the bend of the fold axis, suggesting that structural deformation follows the pre-existing structural trend. Strain distribution in the Jurassic succession increases toward the fold hinge, resulting in the highest fracture intensity. Utilizing the Discrete Fracture Networks (DFNs) model, the N-S trending joint (tension) fracture set follows regional stress associated with the Surat Basin subsidence. Other fractures are strongly controlled by localized stress influenced by the pre-existing MTF.

KEYWORD: Pre-existing Structure, Fracture System, Bowen and Surat Basins

1. Introduction

Pre-existing structures can influence the spatial distribution and geometry of subsequent fractures in sedimentary basins (Phillips et al., 2016; Wang et al., 2023). The occurrence mechanism of these fracture orientations and intensity may be due to local stress changes near pre-existing structures, which modify stress paths and are indicated by local strain axes (Bourne & Willemse, 2001; Maerten et al., 2002; Morley, 2010). This study focuses on the influence of pre-existing structures on fracture systems in Bowen and Surat Basins, eastern Queensland, the Early Permian to the Middle Triassic Bowen Basin is unconformably superimposed by the Surat Basin. The Early-Middle Jurassic successions in the Surat Basin (Figure 1), particularly the Precipice sandstone formation, have theoretical potential as CO_2 sequestration reservoirs (Bradshaw et al., 2011). Given the urgent need to address CO_2 emissions, understanding the storage capacities and seal integrity of these formations is essential. However, the development of fractures in potential reservoirs and seals, which are often affected by pre-existing structures in Bowen Basin, poses a risk for CO_2 leakage.

Beneath the eastern margin of the Bowen and Surat Basins, fold and thrust structures related to the New England Orogeny formed as pre-existing structures before the thermal subsidence phase and the deposition of the reservoir succession in the basin (Exxon, 1976; Korsch et al., 2009).

Due to its wide structural depression, the Surat Basin facilitates long-range CO_2 migration along its gently sloping flanks. A relatively extensive potential storage area has been identified within the Surat Basin (Bradshaw et al., 2011). This makes the basin an appealing option for geological CO_2 storage, especially since most major stationary CO_2 emission sources are situated within 0–300 km of the identified storage area.

This study aims to interpret 3D seismic data and construct a fracture model in the Jurassic rock formation. It focuses on understanding the influence of pre-existing structures on the development of Jurassic to present fracture systems and discussing the potential for CO_2 leakage. This understanding is crucial for ensuring effective and safe CO_2 sequestration, helping to mitigate future pollution and climate change impacts in eastern Queensland, Australia.

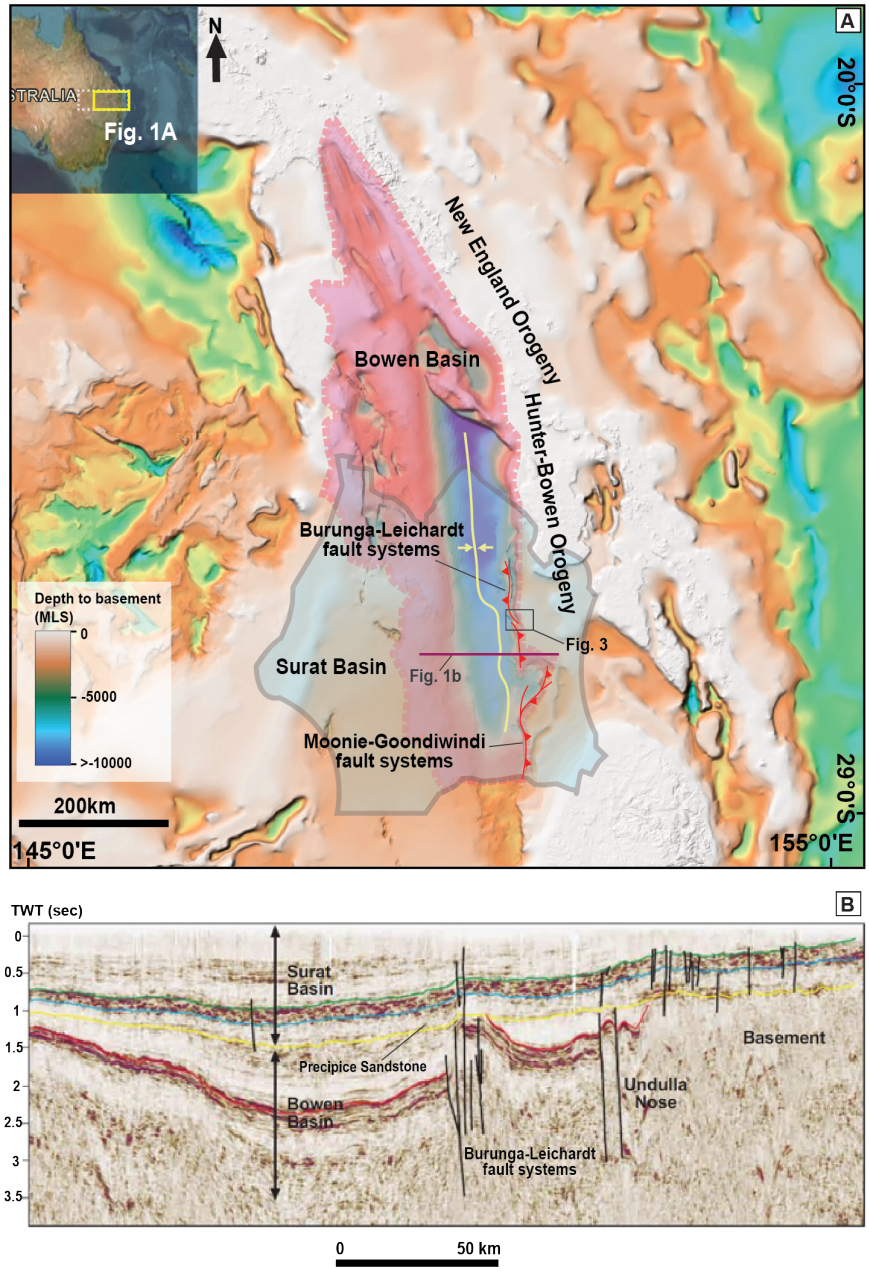

Figure 1. (previous page). (A) Basement depth map showing the pre-existing Bowen basement faults and structures elements of the Burunga-Leichardt and Monie-Goondiwindi fault systems in Bowen Basin that are affected by the Hunter and Bowen Orogeny (modified from Babaahmadi et al., 2017; He et al., 2021). (B) East-west oriented composite seismic line (BMR 84–14), showing the major structural elements and stratigraphy (modified from Martin et al., 2013).

2. Geological background

2.1. Bowen and Surat Basins

The Bowen Basin covers a substantial area, stretching over 1,000 km in length and 250 km in width, with its southern half overlain by the Surat Basin (Figure 1). This basin experienced deformation due to a foreland fold and thrust belt, resulting in a north-south elongated trough and ridge structure (Babaahmadi et al., 2017; He et al., 2021). During the Middle Devonian to the Cretaceous periods, Eastern Australia, which was part of

Eastern Gondwanaland, was located at an active convergent plate margin influenced by a west-dipping subduction system. The Bowen Basin, which formed from the Early Permian to the Middle Triassic, developed in response to tectonic events associated with this active subduction margin. The Surat Basin, formed from the Early Jurassic to the Early Cretaceous, overlies the Bowen Basin (Figures 1b and 2) (Babaahmadi et al., 2017; Korsch et al., 1998; Korsch et al., 2009).

The Bowen Basin features a maximum sediment thickness of around 10 km, with the foreland basin fill mainly located in north-trending depocenters (Dickins & Malone, 1973; Elliott, 1989; He et al., 2021; Totterdell et al., 2009). Two major fault systems, the Burunga-Leichardt and Moonie-Goondiwindi Fault Systems, are situated along the Taroom Trough (Figure 1; He et al., 2021). The Surat Basin is an intra-cratonic sag basin in a thermal subsidence phase, formed during the Jurassic to Cretaceous periods. It spans 327,000 km² and contains up to 2,500 m of nearly flat-lying sedimentary rocks, mainly comprising Jurassic clastic continental sedimentary rocks and Lower Cretaceous marine beds (Exxon, 1976).

2.2 Tectono-stratigraphy

Previous studies suggest that the Bowen Basin began during an extensional phase in the Early Permian period (Figure 2; Babaahmadi et al., 2017; He et al., 2021; Holcombe et al., 1995; Korsch et al., 2009; Rosenbaum, 2018). This phase resulted in the deposition of fluvial and lacustrine sediments, along with Camboon volcanic rock units in the eastern half-grabens, while the western region saw thick layers of coal and nonmarine clastics accumulating within the Lower Back Creek Group. This was followed by a period of thermal subsidence from the Middle to Late Permian, marked by a basin-wide transgression that deposited predominantly clastic sediments, including deltaic and shallow marine formations and extensive coal measures within the Upper Back Creek Group. In the Late Permian, the Bowen Basin was influenced by the Hunter and Bowen Orogeny (Figure 1), an orogenic phase that caused contractional deformation in eastern Australia from the Late Permian to the Middle Triassic periods. This led to the creation of a foreland fold and thrust belt in the Bowen Basin (Figure 2), accelerating subsidence from east to west. This process resulted in a substantial succession of marine and fluvial clastics, accompanied by coal deposits in the Backwater Group, followed by the deposition of fluvial and lacustrine clastic units, including the Lower Triassic Rewan Group, Middle Triassic Clematis Group, and Moolayember Formation during the Early to Middle Triassic. The final stage of the Hunter-Bowen Orogeny involved extensive uplifting, folding, and westward-propagating thrusts, leading to the cessation of sediment deposition in the Bowen Basin during the Middle to Late Triassic period (Cadman et al., 1997; Dickins & Malone, 1973; Elliott, 1989; Green et al., 1997; Korsch et al., 1998; Korsch et al., 2009; Totterdell et al., 2009).

The Surat Basin contains widespread fluvial sandstones and thick, shallow marine-lacustrine shales and siltstones from the Evergreen Formation, along with fluvial-lacustrine siltstones, mudstones, argillaceous sandstones, and regional coal measures from the Walloon Sub-group and Injune Creek Group. During the Jurassic-Cretaceous period, tectonic movements ceased, and the basin entered a thermal subsidence phase. This phase resulted in the formation of the Surat Basin, characterized by virtually flat-lying sedimentary rocks, mainly Jurassic clastic continental sedimentary rocks and Lower Cretaceous marine beds. The basin forms a broad structural depression due to movements related to isostatic readjustment, with limited activity along old fault lines, down warping in areas of sediment accumulation, and draping over basement rises. Additionally, epeirogenic movements in the Late Jurassic and mid-Tertiary caused broad tilting to the south and west and minor movements along old faults in the Surat Basin (Exxon, 1976).

2.3. Structures related to Hunter-Bowen Orogeny

According to Hunter-Bowen Orogeny, this contractional deformation occurred in folding, thrusting, regional uplift, and major fault systems, including Goondiwindi-Moonie Faults and Burunga-Leichardt fault systems (see in Figure 1a; He et al., 2021). The seismic data in the study area consists of rock succession in the Bowen and Surat basins from the Permian-Jurassic period (Figure 2). The study area covers the part of the single large Mimosa Syncline and the Leichhardt- Burunga fault system, which was the main structure during the Late Triassic. Fault in the Jurassic section, with a series of normal faults along the western side, is the target of this study (Babaahmadi et al., 2017; Gonzalez et al., 2019; He et al., 2021).

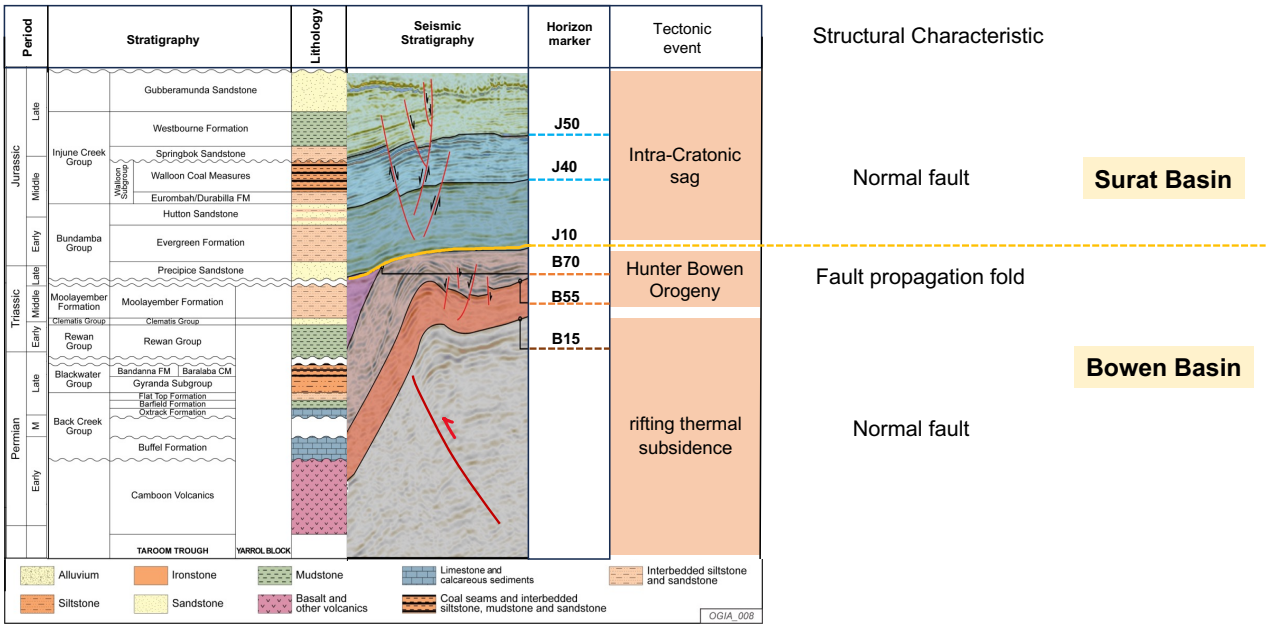

Figure 2. Stratigraphic framework of the Bowen and Surat Basins showing key seismic horizons, major tectonic events, and structural characteristics (modified from Babaahmadi et al., 2017; He et al., 2021; Korsch et al., 2009)

3. Datasets and Methodologies

3.1 Datasets

3.1.1. Seismic data

This study used the southern portion of the Dalwogan-Condabri 3-D seismic data (DC3D; Figure 3), acquired in 2013, covering an area of about 90 km² with the seismic cube-oriented north-south. The dataset is in the MGA94 projection, UTM zone 56S, with a seismic reference datum of 400 m above sea level. The seismic data maintains good quality up to a depth of approximately 1 km within the Jurassic Surat Basin. However, below this depth, the quality of the seismic data deteriorates significantly, particularly within the Permian Bowen Basin.

3.1.2. Well data

In the study area, few wells have been drilled to this stratigraphic level in the Base of Surat and Bowen Basins. There are three deep wells to define downward to the Permian unit, including Miles 1, Condabri Deep 4, and Dalwogan 12 (Figure 3).

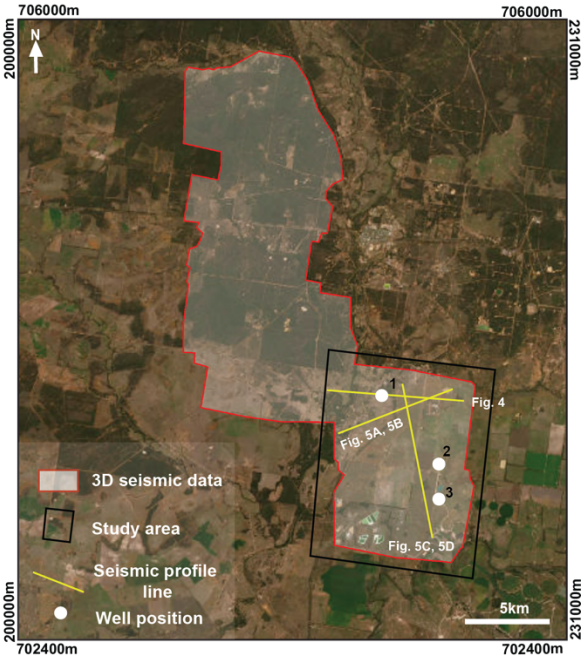

Figure 3. The location and position of the seismic data, with the study focusing on the southern part of the area. This region, covering approximately 90 km², was selected due to its better-quality seismic reflectors and complex structural geology. (1) Miles 1, (2) Dalwogan Deep 4, (3) Dalwogan 12.

3.2. Seismic Interpretation

The seismic interpretation was undertaken using Petrel software. Initially, seismic data is enhanced to improve seismic reflectors for clear interpretation. Then, seismic packages are defined by observing distinctive seismic characteristics correlated with key geological markers and identifying fault systems and structural styles in the study area.

3.3. Depth Conversion

The velocity model was utilized to convert seismic data from the two-way time (TWT) domain to the depth domain. In the Surat part, this conversion spans from the Base Jurassic unconformity to the Earth's surface, using the interval velocity model, which is compared with TvD (time to depth) curves from well data at constant time intervals of every 100 milliseconds. In the Bowen part, the average velocity from the Pre-Stack Time Migration (PSTM) velocity cube was used for the conversion without comparing it to well data (Origin Energy, 2015). The key surfaces in the depth domain were utilized for constructing strain analysis and fracture modeling in MOVE software.

3.4. Relative geological time modeling

The Relative Geological Time (RGT) model is derived from a comprehensive seismic interpretation technique. This technique involves computing a signal-driven grid by creating horizon patches at peaks, troughs, zero-crossings, and inflection points of amplitudes. These patches are tracked by correlation throughout the entire volume. Subsequently, a relative age is assigned to each horizon to define the final model. Once the model is obtained, a volume of dense horizons can be created based on its relative geological times. The signal extraction on each of these horizons enables straightforward mapping of various attributes.

3.5. Structural Restoration and Strain Analysis

A 3D strain simulation was conducted using MOVE software and shown the example procedure of pre-existing Bowen structure strain modeling. First, surfaces from petrel software were inputted to calculate the strain associated with anticline deformation. The anticline restoration was undertaken in three stages. Initially, restoration overburdens surfaces by using 3D kinematic modeling tools. In the second stage, the anticline structure on the Permian Coal surface was restored by using mesh surfaces with 3D geomechanical modeling, which uses a mass-spring algorithm, and strain is tracked during the restoration process. The last stage was strain capture, which collects strain on a geocellular volume.

3.6. Discrete Fracture Networks (DFNs) Modeling

The Discrete Fracture Networks (DFNs) model is the method that is used to predict fracture set distribution in thrust-related anticline folding and extension normal faults in Bowen and Surat Basins by utilizing calculated strain from geomechanical modeling and strain value to define fracture intensity and predicted orientation.

4. Results

4.1. Seismic interpretation

4.1.1. Seismic stratigraphy

In the study area, there are only a few wells that have been drilled from the Surat to the Bowen Basin, with two deep wells, Miles 1 and Condabri Deep 4, providing crucial information about the Permian unit. The prominent reflections (Figure 4) were analyzed using well data and interpretations from Babaahmadi et al. (2017), He et al. (2021), Korsch et al. (2009), and Origin Energy (2015), focusing on six main reflectors. These include the Top Walloon Coal Measures (J50), known for its initial high-amplitude coal and continuous reflection, and the Base Walloon Coal Measures (J40), indicated by the change from high to low amplitude.

The Base-Surat Unconformity (J10) is a confidently identified angular unconformity. The Top Permian (B70) is characterized by high amplitude, representing coal-rich fluvial systems below the Base-Surat Unconformity. The Base Baralaba Coal Measure (Backwater Group; B55) is distinguished by the change from high to low amplitude. The Base Permian (B15) is correlated with reflectors from the Burunga 1 well, located around 80 km to the north (Origin Energy, 2015).

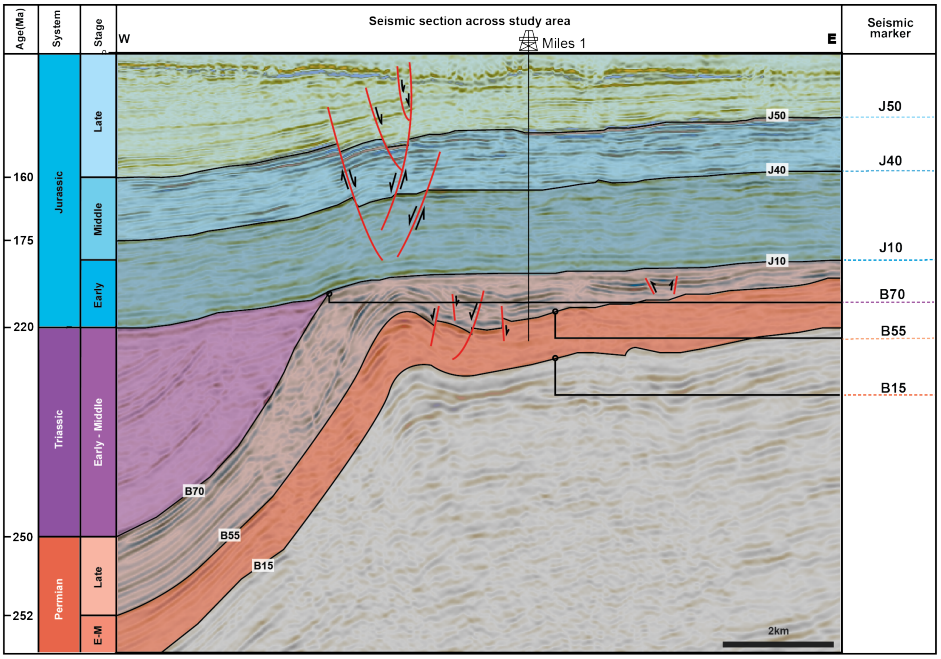

Figure 4. Seismic profile showing key seismic horizons including Top Walloon Coal Measures (J50), Base Walloon Coal Measure (J40), Base-Surat unconformity (J10), Top Permian (B70), Top Baralaba Coal measure (Backwater group; B55), and Base Permian (B15). See Figure 3 for line location.

4.1.2. Structural characteristics beneath the J10 horizon

The seismic profiles reveal that key structures are highlighted, including the Miles Thrust Fault, which is a thrust fault propagating to the hanging wall anticline folding in a westward direction (Figures 5A and 5B), and flower structures (Figures 5C and 5D) that are oblique and perpendicular on the anticline fold hinge.

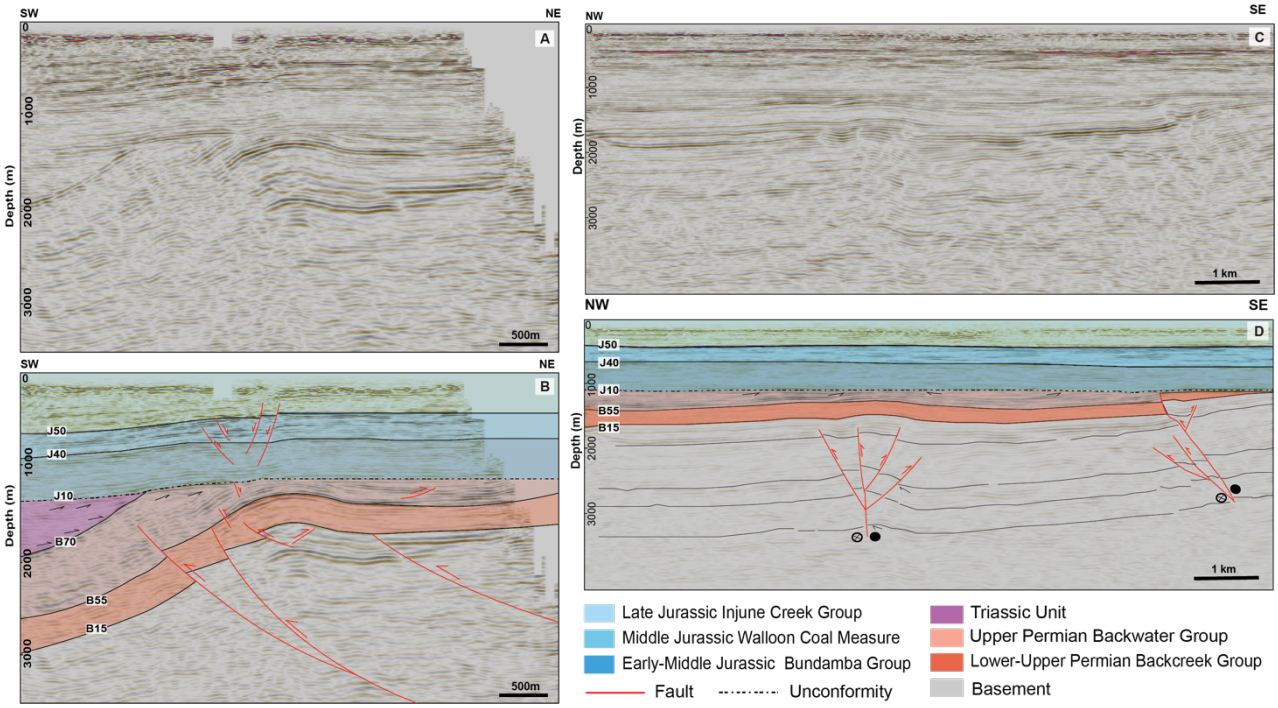

Figure 5. (A) Uninterpreted and (B) interpreted seismic profiles showing the interpretation of the Miles Thrust Fault, which was a thrust fault propagation anticline folding. (C) Uninterpreted and (D) Interpreted seismic profiles showing the interpretation of strike-slip faults and positive flower structures in the central and southern plunge of the anticline, which represented a sinistral movement. The location of the seismic profile is shown in Figure 3

The structural maps, based on two main reflectors, B55 and B15 (Figure 6), reveal the predominant structural style in the study area. The results show that the Miles Thrust Fault causes anticlinal folding, trending in a NNW-SSE direction. Synthetic and antithetic isolated faults propagate displacement along the Miles Thrust Fault.

Additionally, an examination of the geometry of the hanging wall anticline above the Miles Thrust Fault shows dimensions of approximately 9 km in length and 2.5 km in width, oriented in an NW-SE direction. The westward forelimb features a high dip angle, transitioning abruptly through a hinge zone to the eastward backlimb, which has a low dip angle (Figures 5A and 5B). This anticline folding is interrupted by the presence of strike-slip faults, which are controlled by pre-existing structures at depth. These faults exhibit sinistral deformation, indicated by small fault segments displaying a right-stepping en echelon fault pattern, the offset of the anticline fold hinge, and a sharply defined E-W strike-slip fault (Figure 6).

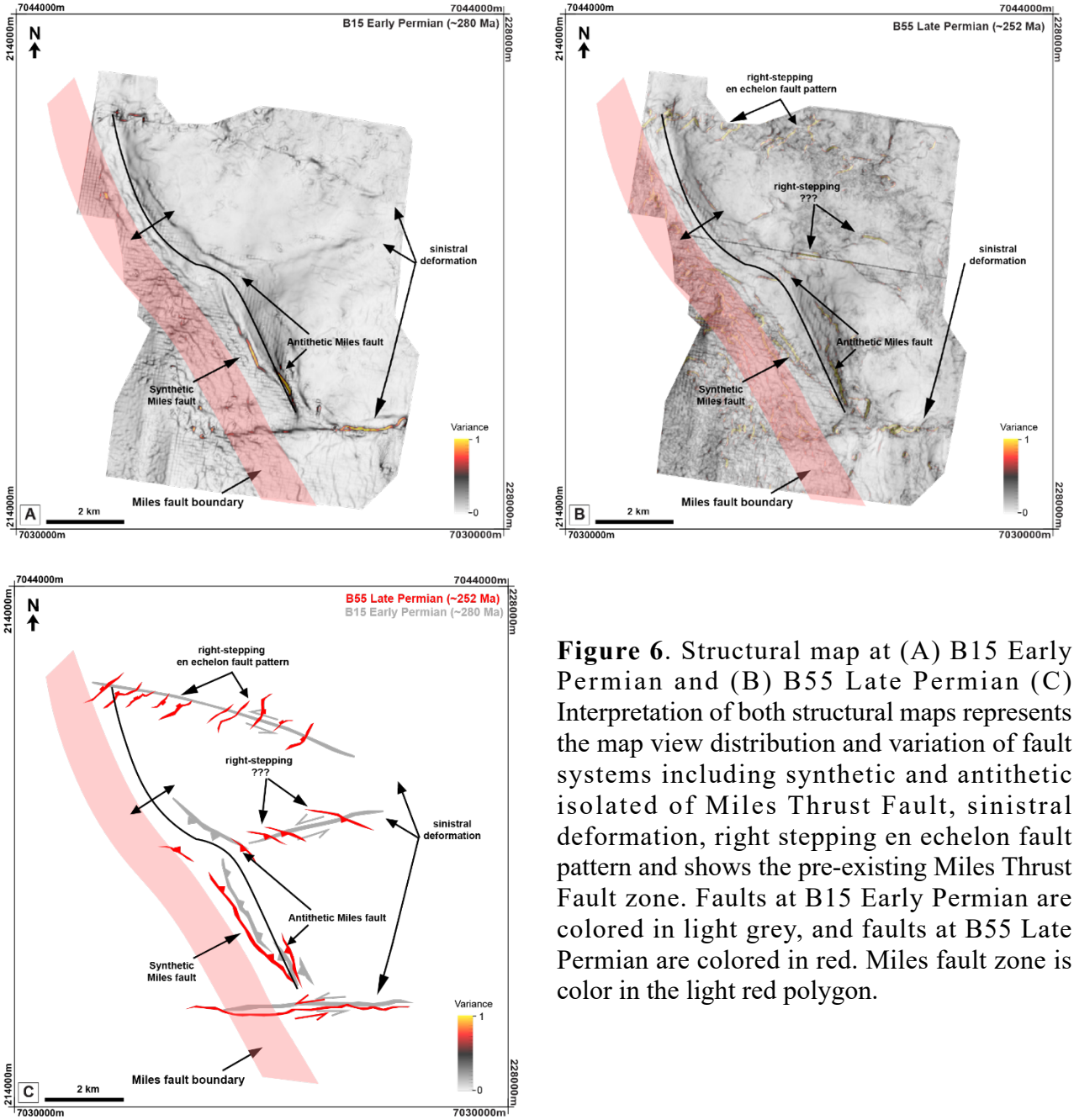

Figure 6. Structural map at (A) B15 Early Permian and (B) B55 Late Permian (C) Interpretation of both structural maps represents the map view distribution and variation of fault systems including synthetic and antithetic isolated of Miles Thrust Fault, sinistral deformation, right stepping en echelon fault pattern and shows the pre-existing Miles Thrust Fault zone. Faults at B15 Early Permian are colored in light grey, and faults at B55 Late Permian are colored in red. Miles fault zone is color in the light red polygon.

4.1.3. Structural characteristics in the Surat Basin (above the J10 horizon)

According to relative geological time modeling, faults in the Surat section are a series of normal faults along the eastern side that were generated in the Jurassic period.

The study area was mainly found as an extensional normal fault characterized by a consistent NW-SE strike orientation along the western part of the study area (see Figure 5), the normal faults oriented in the NNW-SSE direction with NNE and SSW dipping, particularly within the Walloon Coal Measure rock unit. The J10 early Jurassic surface reveals the development of small normal faults, approximately 1 to 2 km on the northern side (Figure 7A), above the Miles Thrust Fault (MTF). The J40 and J50 middle Jurassic surfaces (Figures 7B and 7C) show prominent

NW-SE trending conjugate normal faults, approximately 2 km on the northern side. The southern side shows the longest normal fault, approximately 4 km in length, oriented in an NW-SE direction with a SW dip, which is consistent with the synthetic isolated fault segment of the MTF. Additionally, small normal faults, approximately 200 m in length, oriented NW-SE with a NE dip, are consistent with the antithetic isolated fault segment of the MTF. There is no fault development in the tertiary unconformity surface (Figure 7D).

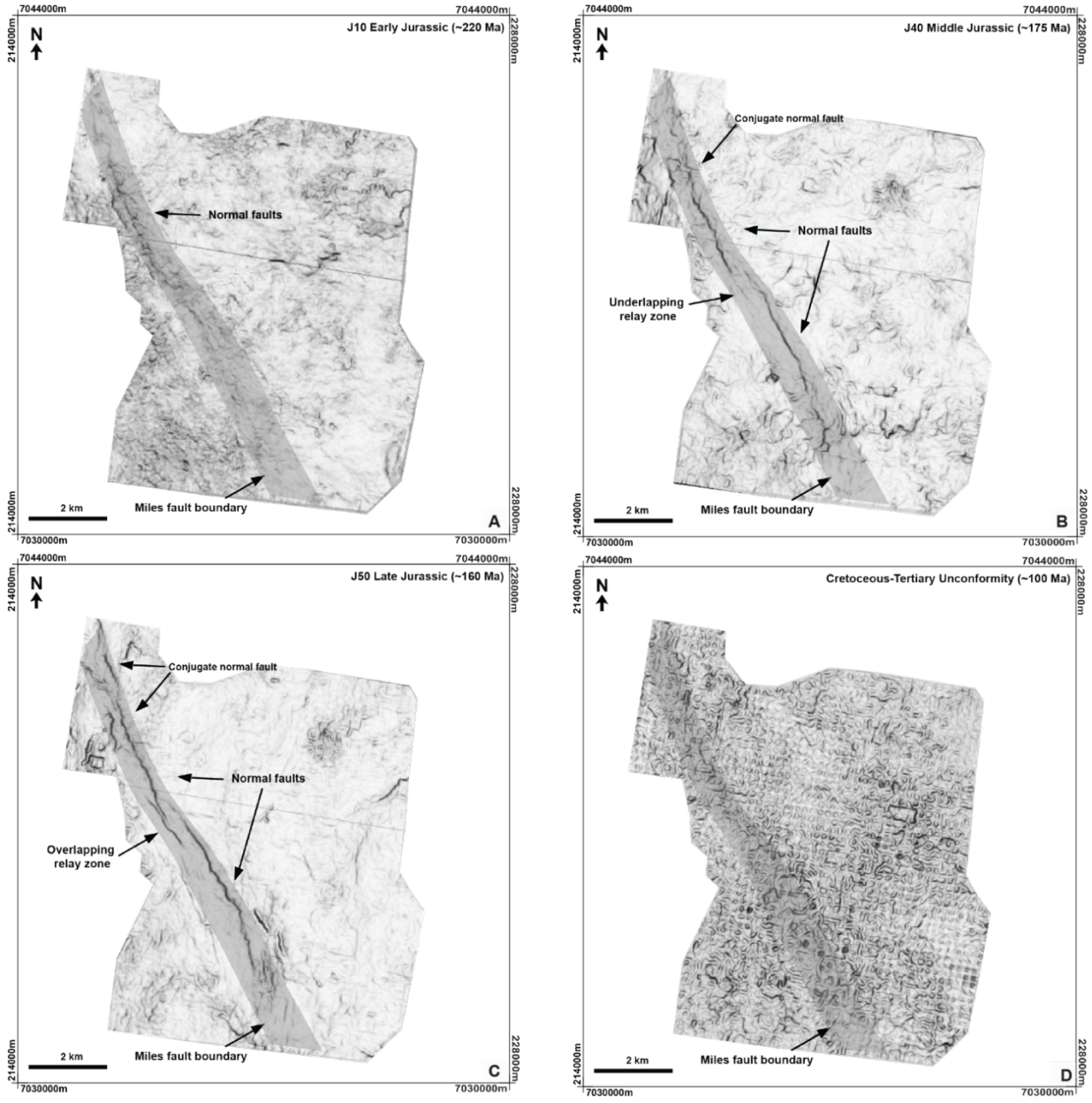

Figure 7. (A) Structural map at the J10 Early Jurassic surface (B) Structural map at the J40 middle Jurassic surface (C). J50 Late Jurassic represents the map view distribution of fault systems, including the normal fault that is influenced by the pre-existing Miles Fault zone. (D) Structural map at Cretaceous-tertiary unconformity surface with no fault appearance. The mile fault zone is colored in the light grey polygon.

4.2. Strain analysis

The results of strain analysis are based on horizons interpreted in both the Bowen and Surat Basins. For the pre-existing Bowen structures, 3D strain modeling on the Bowen surface indicated strain distribution on the folding geometry. For the Surat structures, 3D strain modeling was conducted to indicate strain distribution on the extensional normal fault.

4.2.1. Pre-existing Bowen structure associated strain distribution and modeling

This study used the B55 Late Permian surface (Figure 8A) to determine the 3D strain distribution on the pre-existing Bowen structure, representing the influence of the pre-existing MTF propagating anticline folding.

Principal finite strains perpendicular to anticline fold hinge

The analysis of the finite strain distribution perpendicular to the anticline folding (Figure 8B) reveals the direction of maximum principal strain. In the northern anticline folding, which exhibited the highest strain region, the forelimb was associated with the unfolding of a region with high simple curvature. An abrupt decrease in strain was observed through the fold hinge into the back limb, where the low strain corresponded to low back limb simple curvature. Conversely, the southern anticline folding exhibited a high strain distribution in the forelimb, albeit less than that of the northern folding. This discrepancy resulted from the forelimb in the southern region having lower curvature compared to the northern forelimb. Additionally, the hinge and backlimb of the southern anticline folding showed low strain, corresponding to the low curvature of the backlimb.

Principal finite strains parallel of anticline fold hinge

The analysis of the finite strain distribution parallel to the anticline folding reveals a negative strain, indicating a compressive zone (Figure 8C). This zone is distributed along the fault zone, as depicted in the structural map (Figure 6B). The strain is oriented in a WSW-ENE trend, corresponding to the en-echelon fault pattern in the Northern fold and strike-slip fault in the center and southern regions of the folding.

Principal finite strains perpendicular vertically to anticline fold

The results indicate that in the finite strain distribution perpendicular vertically to the anticline folding, the highest strain region is observed on the northern forelimb, with high strain also observed on the southern forelimb, albeit less than that of the northern forelimb (Figure 8D). The finite strain values are correlated with the curvature of the anticline folding, where regions with high curvature exhibit a high strain distribution.

4.2.2. Jurassic Surat strain analysis

The J50 surface was used to construct the three-dimensional strain modeling of the Jurassic Surat structure that represents the strain distribution along a series of normal faults. Figure 9 shows the Surat structure at depth; it is found that the extensional normal fault at 400 m at depth is oriented in an NW-SE striking with NE-SW dipping.

The extensional normal fault was restored through geomechanical modeling using MOVE software. The calculated strain distribution was color-mapped onto the surface (Figure 9). Analysis of the finite strain distribution reveals the maximum principal strain. The northern side demonstrates the highest strain distribution due to the high deformation of the conjugate fault zone. Additionally, on the central and southern sides, there is a high strain distribution along the main normal faults, which are oriented in an NW-SE trending with SW dipping, and the small normal faults are oriented in an NW-SE trending with NE dipping.

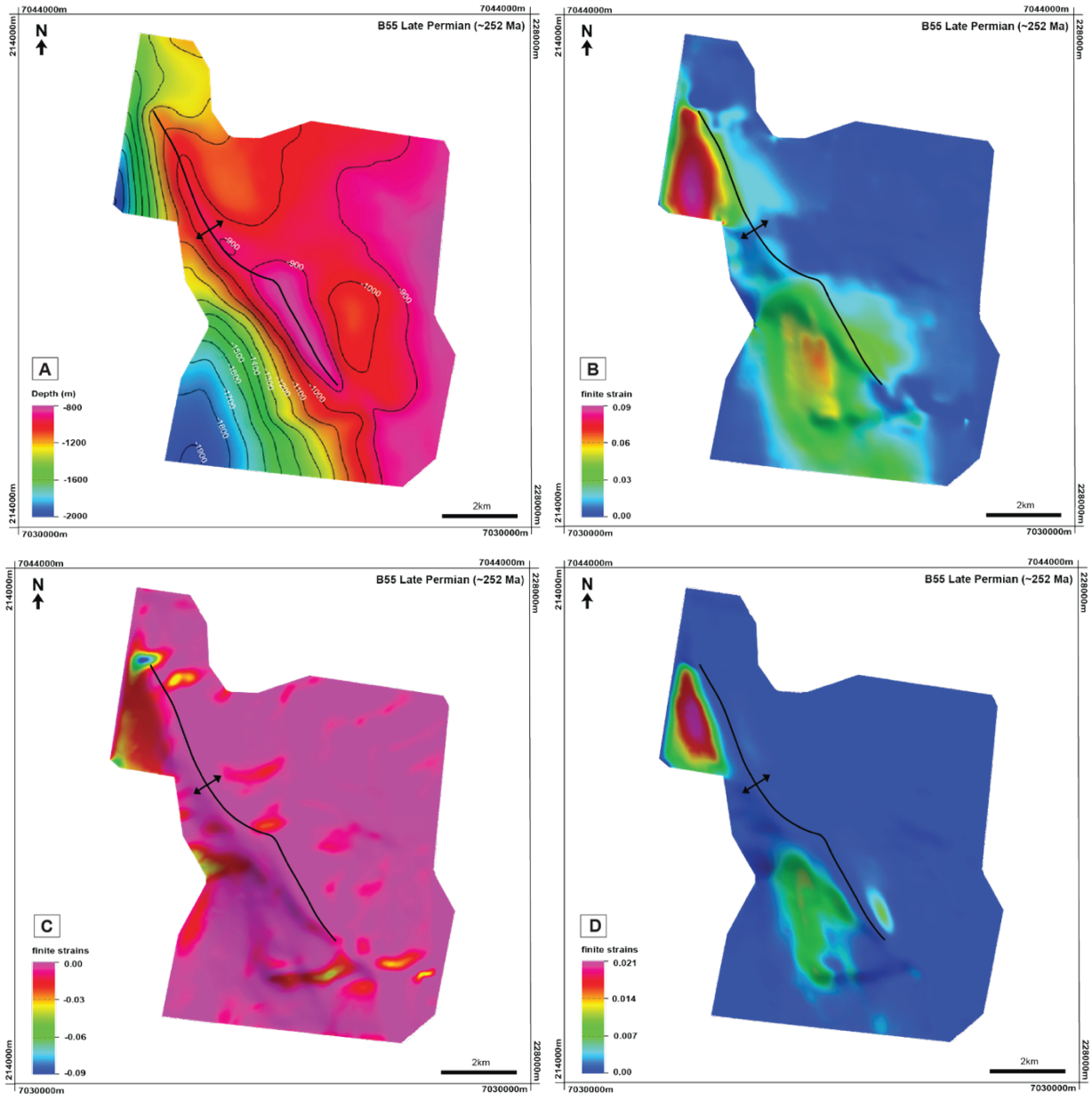

Figure 8. (A) Contour map of anticline folding, (B) Strain map showing principal finite strains perpendicular to anticline fold hinge, (C) Strain map showing principal strain parallel to anticline folding, (D) Strain map showing principal strain perpendicular vertically to the B55 Late Permian anticline folding.

4.3. Fracture modeling

4.3.1. Bowen fracture modeling

The pre-existing Miles Thrust Fault (MTF) structure influenced fracture systems in the Bowen Basin. The key structure was anticline fold geometry, which resulted in varied strain and fracture distribution. Strain values and fracture intensity peaked on the forelimb and decreased on the backlimb of the anticline folding. Fracture orientation from the DFN model predicted four fracture sets (Figure 10): joint or tension fracture sets including J1 (parallel to fold hinge) and J2 (perpendicular to fold hinge), and shear fracture sets including S1 and S2 (intersecting the joint fractures).

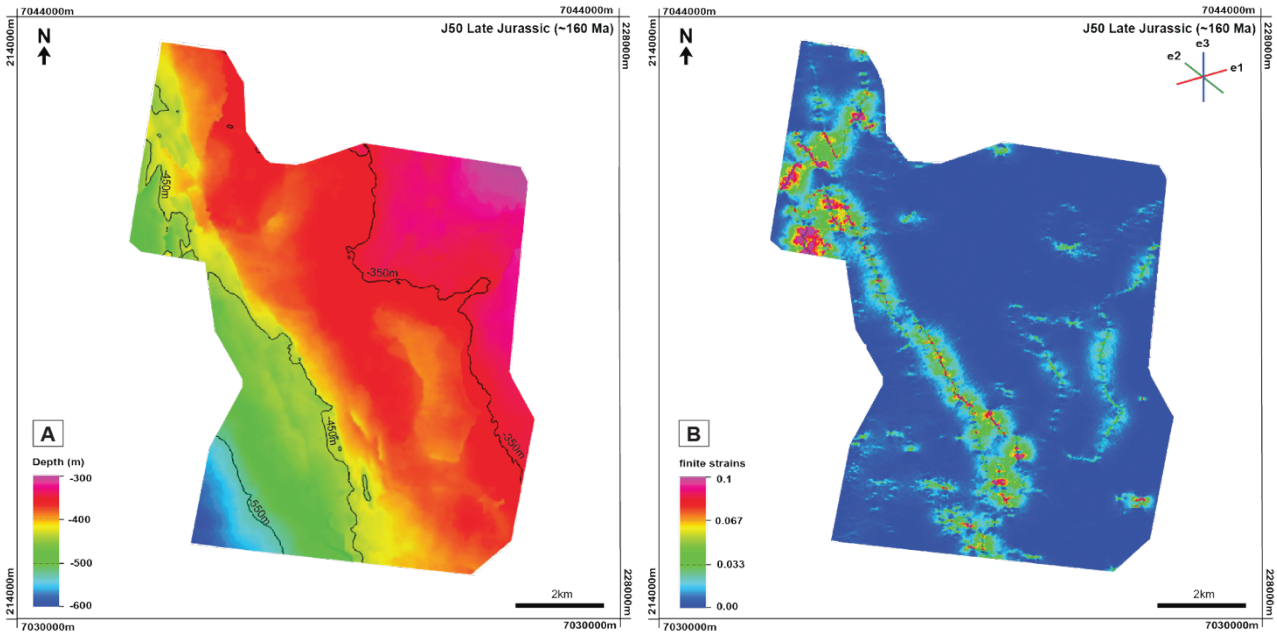

Figure 9. (A) Contour map showing depth surface map of the J50 Jurassic surface. (B) Strain map showing the maximum principal strain of the J50 Jurassic extensional normal faults.

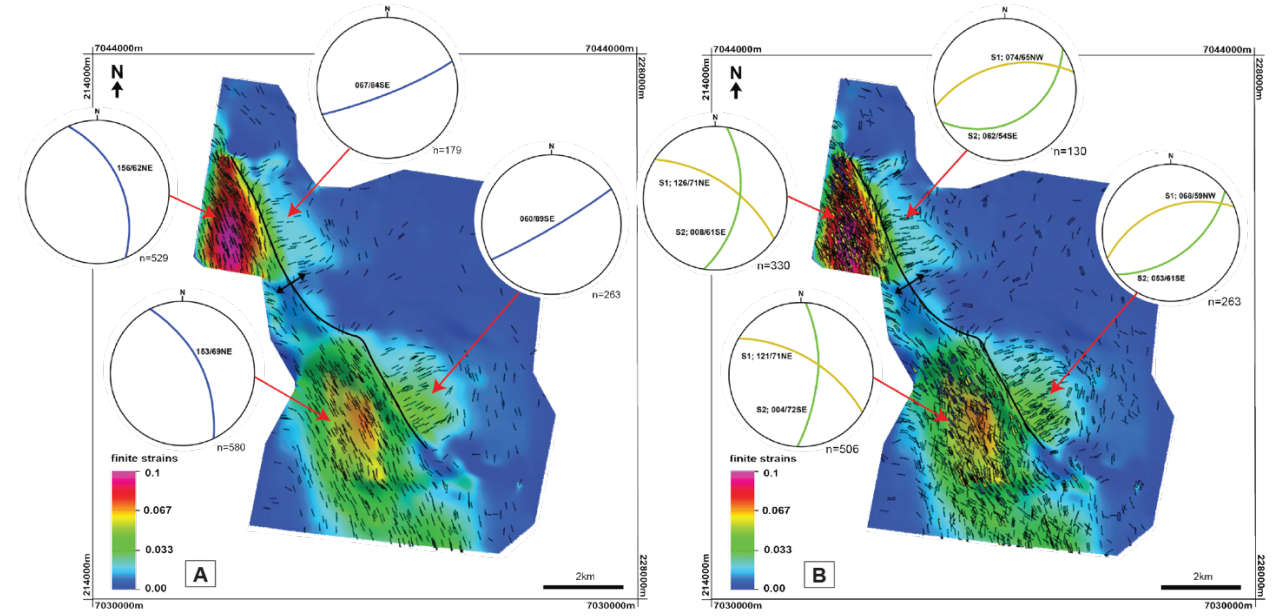

Figure 10. (A) Fracture map showing the predicted fracture distribution and stereo net presenting the predicted fracture orientation on anticline folding. In the forelimb, the fracture set strikes parallel to the fold hinge (J1 fractures), while in the backlimb, the fracture set is perpendicular to the fold hinge (J2 fractures). (B) Fracture map showing the predicted shear fracture distribution and stereonets showing the predicted fracture set orientations, including S1 and S2 fractures occurring in the forelimb and backlimb of folding. Each stereonet shows the mean fracture orientation.

4.3.2. Surat fracture modeling

The pre-existing Miles Thrust Fault (MTF) structure influenced fracture systems in Surat Basins. The major structure was the extensional normal faults, which exhibited high strain values and fracture intensity along their structures. Fracture orientation from the DFN model (Figure 11) predicted an N-S trending joint or tension fracture set following regional stress associated with the Surat Basin subsidence. Other fractures are controlled by localized stress influenced by the pre-existing MTF.

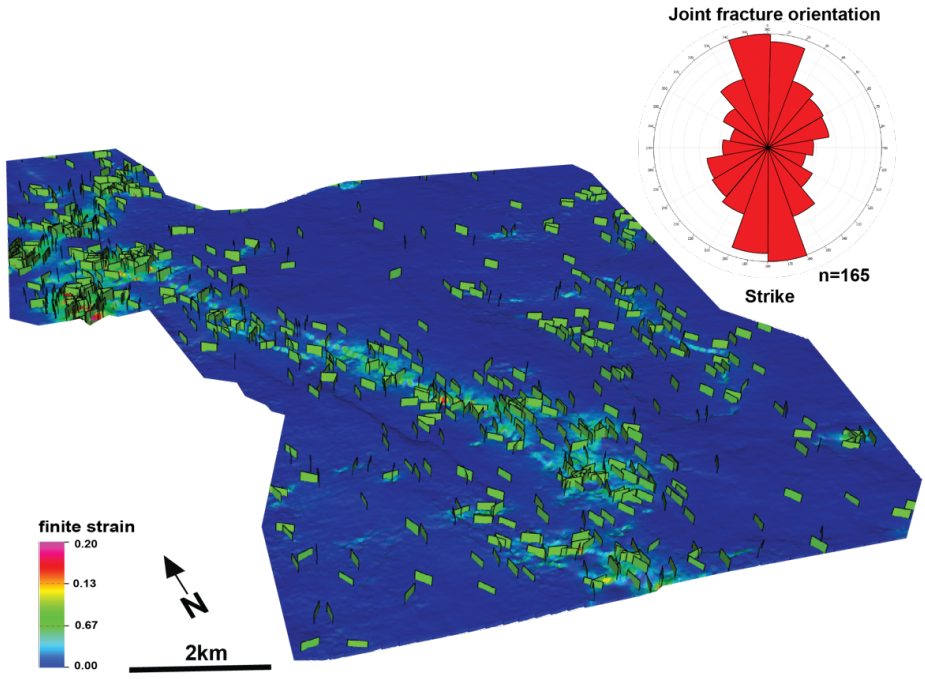

Figure 11. Fracture modeling shows the predicted Surat fracture sets in various orientations and dominantly oriented in N-S striking and occurred along the main Surat normal fault.

5. Discussion

5.1. The influence of pre-existing structure on fracture systems in Bowen and Surat Basins

The pre-existing MTF has significantly influenced the formation of various folding geometries in Bowen Basin and extensional normal faults in Surat Basin, leading to different strain distributions, fracture intensity, and fracture orientation (Figure 12 and Figure 13).

According to Bowen fracture development, the northern fold geometry propagated by the MTF is characterized as an open fold (Fleuty, 1964), and the highest curvature results in the highest strain distribution on the forelimb of the anticline folding (Brandes et al., 2016; Khalifeh-Soltani et al., 2021; Watkins, 2015). There is an abrupt change to lower strain towards the fold hinge and backlimb. Consequently, the highest fracture intensity is observed on the forelimb, where three fracture sets occurred, including J1 tension fractures parallel to the fold hinge and S1 and S2 shear fractures intersecting the J1 tension fractures (Watkins et al., 2018; Watkins, 2015). Conversely, lower fracture intensity is observed in low strain distribution on the back limb, where three fracture sets occurred, including J2 tension fractures perpendicular to the fold hinge and S1 and S2 shear fractures intersecting the J2 tension fractures. In the southern fold geometry, which is propagated by the MTF and characterized as a gentle fold (Fleuty, 1964), there is high curvature in the

forelimb of the anticline folding, although less pronounced than in the northern fold. This results in a lower strain distribution and fracture intensity when compared to the northern fold. However, despite these differences, the fracture sets occur in the same trending sets as observed in the northern fold.

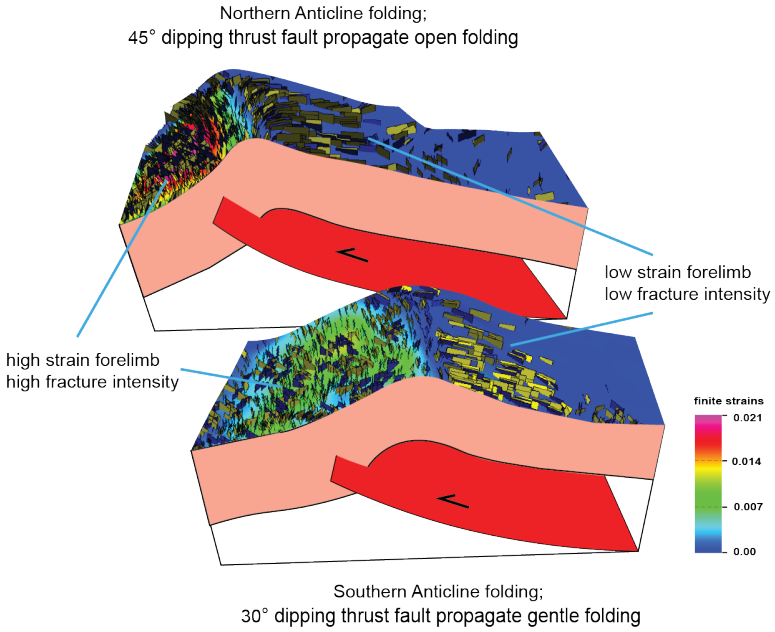

Figure 12. Block diagram showing the pre-existing MTF influence on anticline folding geometries, strain distribution, and fracture intensity area.

The occurrence of fracture sets on the anticline folding in the Bowen Basin is similar to those observed in the Teapot Dome, Powder River Basin, central Wyoming, USA (Cooper et al., 2006), and the Achnashellach fold and thrust belt, NW Scotland (Watkins et al., 2015). In these regions, joint fractures are oriented both parallel and perpendicular to the anticline fold hinge, and conjugate shear fractures are also present along with these joint fractures.

According to fracture development in the Surat Basin (Figure 13), the fractures exhibit considerable variation in orientation, resulting from two controlling mechanisms. The prominent fractures are due to the thermal subsidence mechanism, resulting in fractures oriented in an N-S strike parallel to the depocenter axis in the N-S trending of the Surat Basin subsidence. The other fractures, which deviate from the N-S trend, correspond to the extensional normal fault trending. This is influenced by the pre-existing MTF structure, resulting in the highest fracture intensity along their faults in the Surat Basin.

5.2. Implication for fluid circulation

In normal faults, fracture networks typically exhibit high intensity along the fault zone, with fractures prominently oriented parallel or perpendicular to the fault damage zone (Agosta & Aydin, 2006; Gillam , 2004; Gudmundsson, 2011; Gudmundsson et al., 2010). This pattern is expected to correlate with an increase in permeability or fluid flow leakage pathways. Therefore, areas with high fault and fracture intensity should be treated with caution, especially for Carbon Capture and Storage (CCS) sites (CO2CRC, 2008; Wendt et al., 2022). In the study area, it is advisable to avoid the Surat fault and fracture zones (Figure 13) influenced by the pre-existing MTF structure to prevent CO_2 leakage.

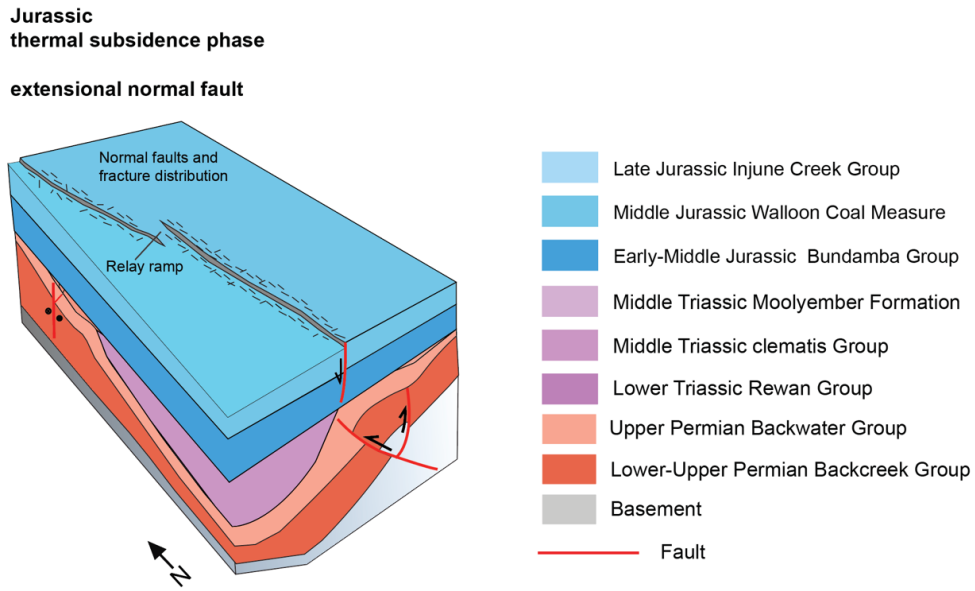

Figure 13. Block diagram showing the Structural and fracture distribution modeling in Jurassic Surat Basin.

6. Conclusion

Based on the comprehensive analysis of seismic interpretation of structures in the study area, as well as the strain model associated with pre-existing structures and fracture distribution linked to the pre-existing Bowen structure and Surat structure, the following conclusions can be drawn:

1. The Miles Thrust Fault (MTF) is a pre-existing structure characterized by folds and thrusts in the Bowen Basin, associated with ~E–W shortening from the Late Permian to the Middle Triassic. The MTF accommodated different displacements in each thrust sheet, causing local strike-slip faults to develop in the hanging wall blocks. The MTF represents a weak zone toward the fold hinge in the Jurassic Surat, leading to the formation of a series of normal faults along this pre-existing fault trend.

2. The analysis of strain distribution in the Surat Basin reveals high strain along extensional normal fault trends, resulting in the highest fracture intensity along these faults.

3. Utilizing the Discrete Fracture Network (DFN) model, the joint (tension) fracture set strikes prominently in an N-S trend parallel to the depocenter axis in the Surat Basin subsidence. Other fractures strike parallel to the Surat extensional normal fault, influenced by the pre-existing Miles Thrust Fault (MTF) structure.

4. For Carbon Capture and Storage (CCS) sites, it is advisable to avoid the Surat fault and fracture zones. These zones are considered cautionary areas due to their influence from the pre-existing structure, which could potentially lead to leakage.

Acknowledgments

I am grateful to the Department of Geology, Faculty of Science, Chulalongkorn University, for providing the necessary knowledge and equipment for this research and thankful to the Development and Promotion of Science and Technology Talents Project for providing me with the opportunity to pursue the Master of Science Program in Geology at Chulalongkorn University and special thanks

are due to the Queensland Government for generously providing seismic data and reports that were instrumental in this research. I am also grateful to Schlumberger, Eliis, and PE Limited (Petex) for their software licenses, which greatly supported my research.

References

Agosta, F., & Aydin, A. (2006). Architecture and deformation mechanism of a basin-bounding normal fault in Mesozoic platform carbonates, central Italy. *Journal of Structural Geology*, *28*(8), 1445-1467.

Babaahmadi, A., Sliwa, R., Esterle, J., & Rosenbaum, G. (2017). The development of a Triassic fold-thrust belt in a synclinal depositional system, Bowen Basin (eastern Australia). *Tectonics*, *36*(1), 51-77.

Bourne, S. J., & Willemse, E. J. (2001). Elastic stress control on the pattern of tensile fracturing around a small fault network at Nash Point, UK. *Journal of Structural Geology*, *23*(11), 1753-1770.

Bradshaw, B. E., Spencer, L. K., Lahtinen, A.-L., Khider, K., Ryan, D. J., Colwell, J. B., Chirinos, A., Bradshaw, J., Draper, J. J., & Hodgkinson, J. (2011). An assessment of Queensland's CO2 geological storage prospectivity—The Queensland CO2 geological storage atlas. *Energy Procedia*, *4*, 4583-4590.

Brandes, C., Tanner, D. C., & Winsemann, J. (2016). Kinematic 3-D retro-modeling of an orogenic bend in the South Limón fold-and-thrust belt, eastern Costa Rica: Prediction of the incremental internal strain distribution. *Pure and Applied Geophysics*, *173*, 3341-3356.

Cadman, S., Pain, L., & Vuckovic, V. (1997). *Bowen and Surat Basins, Clarence-Moreton Basin, Sydney Basin, Gunnedah Basin and Other Minor Onshore Basing, Qld, NSW and NT*. Department of Primary Industries and Energy, Bureau of Resource Sciences.

CO2CRC, S. C. E. (2008). Site Selection and Characterisation for CO2 Storage Projects. *Cooperative Research Centre for Greenhouse Gas Technologies, Canberra, CO2CRC Report No: RPT08-1001*.

Cooper, S. P., Goodwin, L. B., & Lorenz, J. C. (2006). Fracture and fault patterns associated with basement-cored anticlines: The example of Teapot Dome, Wyoming. *AAPG Bulletin*, *90*(12), 1903-1920.

Dickins, J. M., & Malone, E. J. (1973). *Geology of the Bowen Basin, Queensland* (Vol. 130). Australian Government Pub. Service.

Elliott, L. (1989). The Surat and Bowen Basins. *The APPEA Journal*, *29*(1), 398-416.

Exxon, N. (1976). Geology of the Surat Basin in Queensland: Australian Bureau of Mineral Resources. *Geology and Geophysics, Bulletin*.

Fleuty, M. (1964). The description of folds. *Proceedings of the Geologists' Association*, *75*(4), 461-492.

Gillam, D. J. (2004). *Structural and geomechanical analysis of naturally fractured hydrocarbon provinces of the Bowen and Amadeus Basins: onshore Australia/Daniel J Gillam*

Gonzalez, S., He, J., Underschultz, J., & Garnett, A. (2019). Seismic interpretation–geophysics.

Green, P., Hoffmann, K., Brain, T., & Gray, A. (1997). The Surat and Bowen basins, south-east Queensland. *Brisbane: Queensland Department of Mines and Energy*.

Gudmundsson, A. (2011). *Rock fractures in geological processes*. Cambridge University Press.

Gudmundsson, A., Simmenes, T. H., Larsen, B., & Philipp, S. L. (2010). Effects of internal structure and local stresses on fracture propagation, deflection, and arrest in fault zones. *Journal of Structural Geology*, *32*(11), 1643-1655.

He, J., La Croix, A. D., Gonzalez, S., Pearce, J., Ding, W., Underschultz, J. R., & Garnett, A. (2021). Quantifying and modeling the effects of pre-existing basement faults on the folding of overlying strata in the Surat Basin, Australia: Implications for fault seal potential. *Journal of Petroleum Science and Engineering*, *198*, 108207.

Holcombe, R., Fielding, C., & Stephens, C. (1995). Tear fault termination of the fold-thrust belt in the Northern New England Orogen. Geological Society of Australia Abstracts,

Khalifeh-Soltani, A., Alavi, S. A., Ghassemi, M. R., & Ganjiani, M. (2021). Influence of mechanical parameters and overburden pressure on the mechanical evolution of fault propagation folds: insights from 2D finite-element elastic-plastic models applied to the Ayegan anticline, central Alborz. *Geopersia*, *11*(1), 101-114.

Korsch, J., Boreham, C., Totterdell, J., Shaw, R., & Nicoll, M. (1998). Development and petroleum resource evaluation of the Bowen, Gunnedah, and Surat basins, eastern Australia. *The APPEA Journal*, *38*(1), 199-237.

Korsch, R., Totterdell, J., Fomin, T., & Nicoll, M. (2009). Contractional structures and deformational events in the Bowen, Gunnedah, and Surat Basins, eastern Australia. *Australian Journal of Earth Sciences*, *56*(3), 477-499.

Maerten, L., Gillespie, P., & Pollard, D. D. (2002). Effects of local stress perturbation on secondary fault development. *Journal of Structural Geology*, *24*(1), 145-153.

Martin, M., Wakefield, M., MacPhail, M., Pearce, T., & Edwards, H. (2013). Sedimentology and stratigraphy of an intra-cratonic basin coal seam gas play: Walloon Subgroup of the Surat Basin, eastern Australia.

Morley, C. (2010). Stress re-orientation along zones of weak fabrics in rifts: An explanation for pure extension in 'oblique'rift segments? *Earth and Planetary Science Letters*, *297*(3-4), 667-673.

Origin Energy. (2015). Dalwogan Condabri 3D seismic survey interpretation report. https://geoscience.data.qld.gov.au/data/dataset/cr099111/resource/geo-doc962630-cr099111

Phillips, T. B., Jackson, C. A., Bell, R. E., Duffy, O. B., & Fossen, H. (2016). Reactivation of intrabasement structures during rifting: A case study from offshore southern Norway. *Journal of Structural Geology*, *91*, 54-73.

Rosenbaum, G. (2018). The Tasmanides: Phanerozoic tectonic evolution of eastern Australia. *Annual Review of Earth and Planetary Sciences*, *46*, 291-325.

Totterdell, J., Moloney, J., Korsch, R., & Krassay, A. (2009). Sequence stratigraphy of the Bowen–Gunnedah and Surat Basins in New South Wales. *Australian Journal of Earth Sciences*, *56*(3), 433-459.

Wang, D., Yang, L., Li, W., & Wang, X. (2023). The Impact of Pre-Existing Faults on Fault Geometry during Multiphase Rifts: The Jiyang Depression, Eastern China. *Journal of Marine Science and Engineering*, *11*(10), 1971.

Watkins, H., Healy, D., Bond, C. E., & Butler, R. W. (2018). Implications of heterogeneous fracture distribution on reservoir quality; an analogue from the Torridon Group sandstone, Moine Thrust Belt, NW Scotland. *Journal of Structural Geology*, *108*, 180-197.

Watkins, H. E. (2015). *Characterising and predicting fracture patterns in a sandstone fold-and-thrust belt* the University of Aberdeen].

Wendt, A., Sheriff, A., Shih, C. Y., Vikara, D., & Grant, T. (2022). A multi-criteria CCUS screening evaluation of the Gulf of Mexico, USA. *International Journal of Greenhouse Gas Control*, *118*, 103688.